Electrochemical and Solid-State Letters, **13** (8) J92-J95 (2010)
1099-0062/2010/13(8)/J92/4/$28.00 © The Electrochemical Society

Fabrication of Polycrystalline Si Films by Vapor-Induced Crystallization and Rapid Thermal Annealing Process

Yong-Ho Yang,[a,b] Kyung-Min Ahn,[a] and Byung-Tae Ahn[a,*,z]

[a]*Department of Materials Science and Engineering, Korea Advanced Institute of Science and Technology, Daejeon 305-701, Korea*
[b]*Samsung Mobile Display Company, Cheonan 331-300, Korea*

We have developed a crystallization process, where the crystallization temperature is lowered to the conventional rapid thermal annealing (RTA) process and the metal contamination is reduced compared to the conventional vapor-induced crystallization (VIC) process. a-Si film on the seed layer, which was crystallized by the VIC process, was crystallized by the RTA process at 680°C for 5 min. The poly-Si film appeared as a needlelike growth front with a relatively well-arranged Si(111) orientation. Moreover, the Ni concentration in the poly-Si film was reduced to 3×10^{17} cm^{-3}. The reduction in metal contamination could be helpful to achieve a low leakage current in poly-Si thin film transistors.
 [DOI: 10.1149/1.3432320]

Manuscript submitted March 12, 2010; revised manuscript received April 30, 2010. Published May 24, 2010.

Poly-Si thin film transistors (TFTs) are used for flat panel active matrix liquid crystal display panels and active matrix organic light emitting diode (AMOLED) displays. The performance of poly-Si TFTs is influenced by the grain size, grain boundaries, intragranular defects, and impurities. To obtain high quality poly-Si thin films, the crystallization methods of amorphous silicon (a-Si) thin films have been widely studied. Conventional furnace annealing in solid phase crystallization (SPC) usually requires more than 10–20 h for crystallization.[1] To reduce the crystallization temperature and improve the crystallinity of poly-Si film, many methods such as metal-induced crystallization (MIC),[2] vapor-induced crystallization (VIC),[3,4] metal-induced lateral crystallization,[5] field-aided lateral crystallization,[6] microwave-enhanced crystallization,[7] and metal-induced crystallization through a cap[8] have been investigated. However, these crystallization processes usually require more than 5–10 h for crystallization. In addition, cost effectiveness is required for the mass production of flat panel displays, so a rapid thermal annealing (RTA) process has also been developed.[9,10] The RTA process could obtain poly-Si film in a very short annealing time at higher temperatures, but the grain size of the poly-Si film annealed by RTA is much smaller. In the VIC process, $NiCl_2$ vapor was supplied on a-Si, and the crystallization was reduced to as low as 480°C. However, the Ni content in the poly-Si film should be reduced to decrease the leakage current.[4]

In this article, we propose a crystallization process to reduce the RTA process temperature with the help of the poly-Si seed layer grown by the VIC process. The Ni content in the poly-Si film can be further reduced through our process. First, a very thin a-Si film was deposited on a SiO_2 layer and was crystallized using the VIC process. Then, a thick a-Si layer was deposited on the VIC poly-Si film and was crystallized by the RTA process where VIC poly-Si acted as a seed layer. Our process is simply named the (VIC + RTA) process.

Figure 1 shows the schematics of the (VIC + RTA) process used to fabricate poly-Si films in this study. a-Si film was deposited on the thermally oxidized Si wafer by hot-wire chemical vapor deposition (HWCVD) at 500°C using 20% diluted SiH_4 in Ar. In the HWCVD system, a W-shaped tungsten wire of 0.5 mm diameter was positioned 4.5 cm away from the substrate and was heated to approximately 1900°C, as measured by an optical pyrometer. The base pressure was under 1×10^{-6} Torr, and the working pressure was maintained at 10 mTorr. A 5 nm thick a-Si film was deposited and crystallized by the VIC process at 550°C for 3 h. The source temperature of $NiCl_2$ was 500°C and was transported from the source zone to the annealing zone as a vapor phase by N_2 gas flow.[4] After the VIC process, the poly-Si seed layer was dipped in 1.5% HF solution to remove a surface oxide on the seed layer. A 50 nm thick a-Si film was then deposited on the poly-Si seed layer by HWCVD at 500°C using 20% diluted SiH_4 in Ar. This layer is called the top layer. The crystallization of the top a-Si layer was performed by the RTA process at 680°C for 5 min in Ar as an ambient atmosphere.

For a comparison, 50 nm thick a-Si films were deposited on the thermally oxidized Si wafer by HWCVD at 500°C under the same conditions. The a-Si films were then crystallized using the VIC pro-

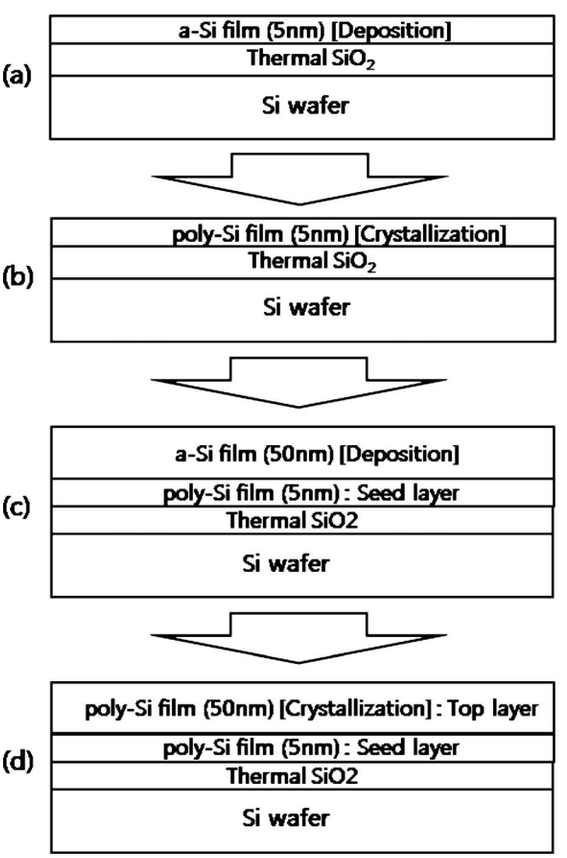

Figure 1. Schematics of (VIC + RTA) process: (a) Deposition of a-Si seed layer (5 nm), (b) crystallization by VIC process (530°C, 3 h), (c) deposition of a-Si top layer (50 nm), and (d) crystallization by RTA process (680°C, 5 min).

* Electrochemical Society Active Member.
z E-mail: btahn@kaist.ac.kr

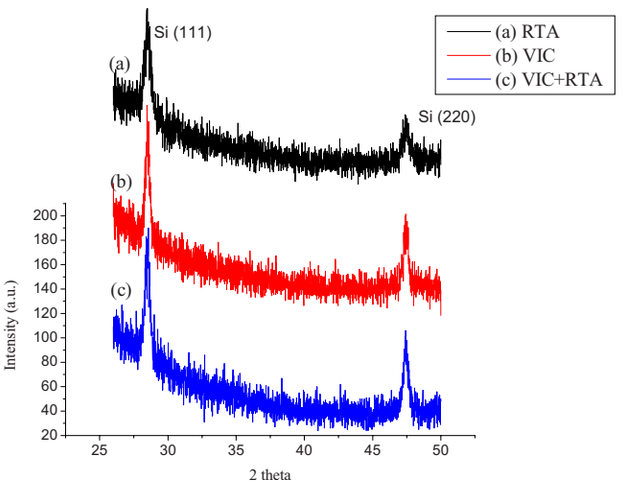

Figure 2. (Color online) XRD patterns of (a) poly-Si film by RTA process, (b) poly-Si film by VIC process, and (c) poly-Si film by (VIC + RTA) process.

cess or the RTA process. The RTA process was carried out at 730°C for 5 min, which was the minimum crystallized temperature under this process. In the VIC process, the crystallization of a-Si films was performed at 550°C for 5 h with $NiCl_2$ source material.

The crystal structure and crystallinity were determined by X-ray diffraction (XRD). The microstructure of samples was characterized by transmission electron microscopy (TEM) operated at 200 kV and scanning electron microscopy (SEM). For SEM grain observation, the remaining a-Si was removed by secco-etching with a solution consisting of CrO_3:49% HF:H_2O = 0.75:1:100. Secondary-ion mass spectroscopy (SIMS) was employed to analyze the distribution of Ni in the poly-Si films.

Figure 2 shows the XRD patterns of (a) poly-Si film produced by the RTA process at 730°C for 5 min, (b) poly-Si film produced by the VIC process at 550°C for 5 h, and (c) poly-Si film produced by the (VIC + RTA) process at 680°C for 5 min. Diffraction peaks of Si(111) positioned at $2\theta = 28.5°$ and Si(220) positioned at $2\theta = 47.4°$ were ascertained. We ascertained full crystallization of a-Si by comparing the time dependence of Si(111) and Si(220) diffraction peaks in each process. In the (VIC + RTA) process, the crystallization temperature of the a-Si top film on the poly-Si seed layer crystallized by the VIC process could be crystallized as low as 680°C, which is 50°C lower than that of a-Si film crystallized by the RTA process alone. The intensity ratios of the Si(111) peak to the Si(220) peak in poly-Si films produced by the RTA, VIC, and (VIC + RTA) processes were 2.17, 1.92, and 1.89, respectively. The intensity ratio of 2.17 by the RTA process is close to that by the furnace-SPC process, which shows a Si(111) preferred orientation due to the twin-assisted grain growth mechanism.[11] The ratios in the poly-Si films produced by the VIC and the (VIC + RTA) process are close to that of the poly-Si powder with random orientation (1.82). In the VIC process, no preferred orientation is shown due to silicide grain growth mechanism.[12] Due to the different grain growth mechanisms, the Si(220) peak intensity with respect to Si(111) for the poly-Si film prepared by the RTA process is lower compared to that prepared by the VIC process. Because the Si(111)/(220) intensity ratio of the (VIC + RTA) process is nearly same as that of the VIC process, it is thought that the (VIC + RTA) process has the same grain growth mechanism as the VIC process has.

Figure 3 shows SEM images of the surface morphology of the poly-Si films produced using various processes. Figure 3a shows a surface SEM image of a poly-Si film crystallized by the RTA process at 730°C for 5 min. The grains in Fig. 3a are very small and irregular, and the feature of a growth direction in grains that can be anticipated was not found. Figure 3b shows the grain's growth when fabricated using the VIC process with $NiCl_2$. The needlelike grains, which are characteristic of the VIC process when using $NiCl_2$, are

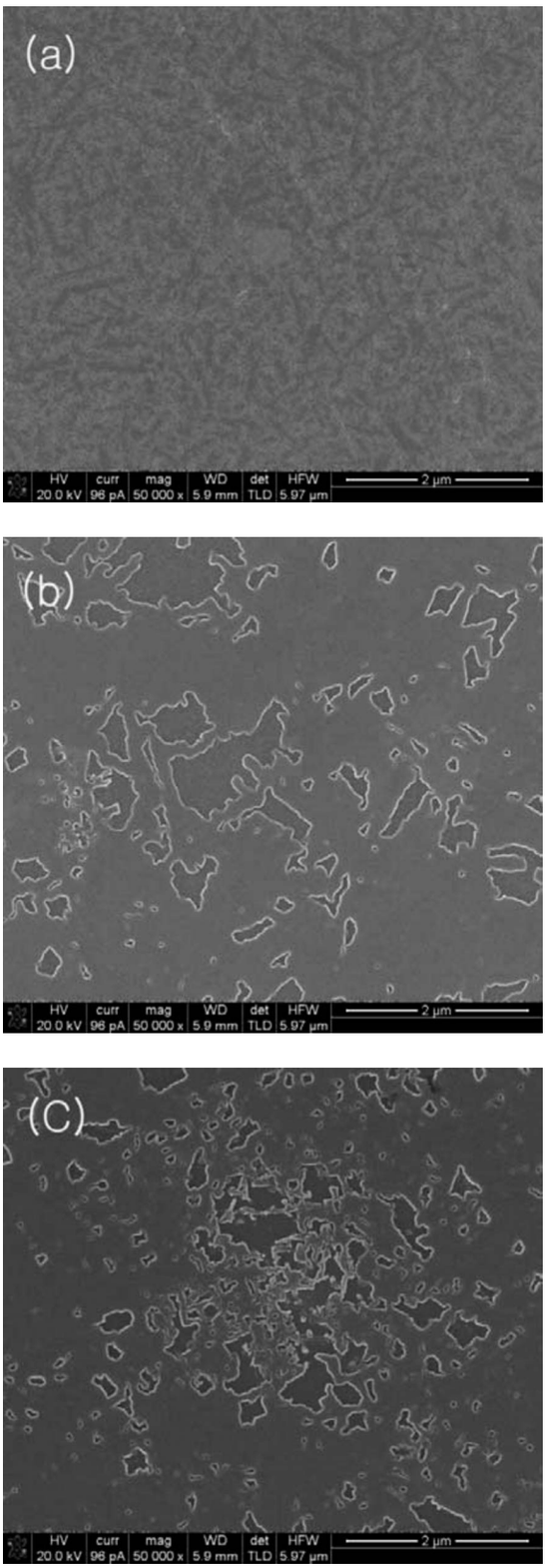

Figure 3. SEM image of surface morphology of poly-Si film after a secco-etching: (a) RTA process, (b) VIC process, and (c) (VIC + RTA) process.

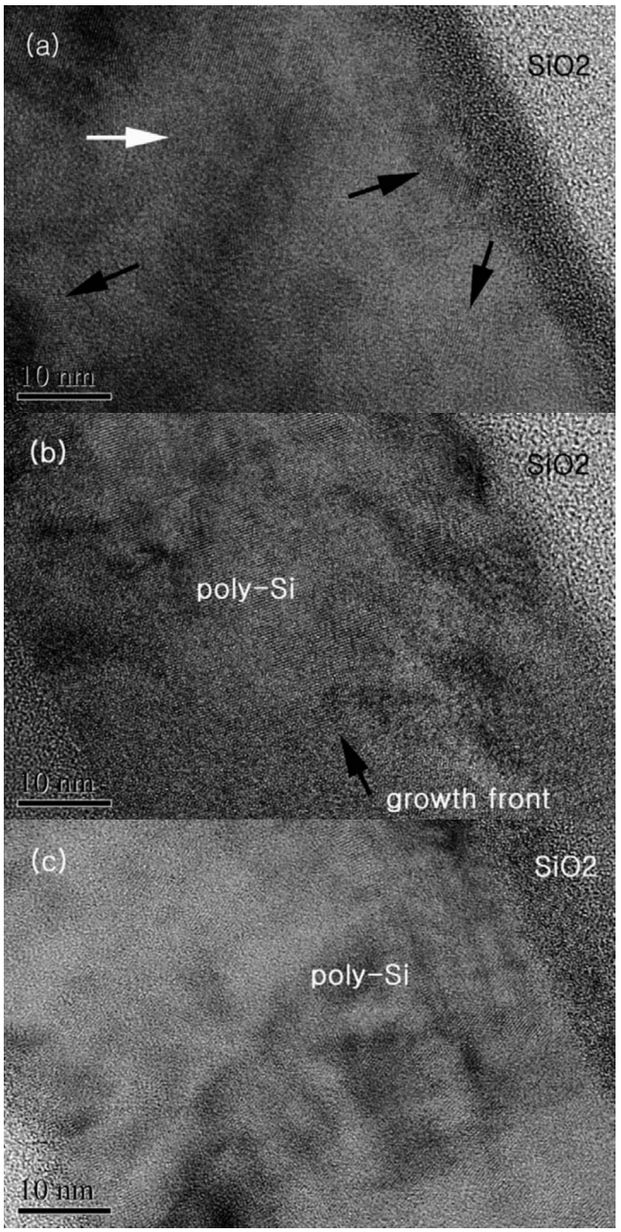

Figure 4. Cross-sectional TEM images of sample with poly-Si/SiO_2 structures: (a) RTA process, (b) VIC process, and (c) (VIC + RTA) process.

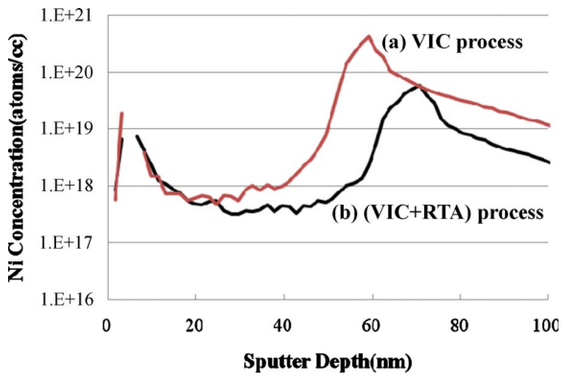

Figure 5. (Color online) SIMS depth profiles of Ni in the poly-Si films crystallized (a) by VIC process and (b) by (VIC + RTA) process.

shown all over the films. $NiSi_2$ precipitates exist only at the tips of the needles and no $NiSi_2$ exists on the sides of the needles.[13,14] Such grain growth is also confirmed in Fig. 3c, which shows a poly-Si film crystallized by the (VIC + RTA) process at 680°C for 5 min. The crystallization temperature when using only the RTA process could not be reduced below 730°C with a-Si film under our HWCVD conditions. Considering the needlelike grains as well as the crystallization temperature of the top layer as produced by the (VIC + RTA) process, it was thought that the top a-Si layer was crystallized with the help of $NiSi_2$ precipitates that originated from the poly-Si seed layer.

Figure 4 shows cross-sectional TEM images of poly-Si films produced by each process. Figure 4a shows a TEM image of the sample with a poly-Si film crystallized by the RTA process. The black arrows indicate the areas of the (111) plane in many parts, and the white arrow indicates the area of the amorphous phase. Grains formed planes with the same direction had a relatively small range and an irregular shape, and the plane's arrangement of each grain was random. Grain size was on the order of nanometers. Figure 4b shows a TEM image of the sample with a poly-Si film crystallized by the VIC process. Both a crystallized area and a growth front can be seen. A Si(111) plane had a well-regulated arrangement and grew in a downward direction, resulting in large grains with fewer defects within the grain. Figure 4c shows a TEM image of the sample with a poly-Si film/SiO_2 buffer layer formed by the (VIC + RTA) process. The planar distance among the 10 layers was about 3.27 nm. Because most of the area in the TEM image showed the formation of an identical arrangement of the (111) plane, it was considered that the grain size could be several tens of nanometers in the poly-Si film.

Considering the aspect of plane arrangements in the TEM image and the needlelike grain in the SEM image, it was thought that the microstructure of poly-Si films produced by the (VIC + RTA) process was analogous to that produced by the VIC process. As a result, although the (VIC + RTA) process applied an annealing process for only 5 min by RTA, the crystalline quality of the poly-Si film was expected to be improved.

Figure 5 show the SIMS depth profile of Ni in the crystallized Si films by (a) the VIC process and (b) the (VIC + RTA) process. In the VIC process, Ni is accumulated at the surface with a peak value of 1×10^{19} cm^{-3} and near the poly-Si and SiO_2 interface with a peak value of 4×10^{20} cm^{-3}. The Ni concentration in the middle range of the poly-Si film is in the range of 6×10^{17} to 1×10^{18} cm^{-3}. In the (VIC + RTA) process, the Ni concentration in the middle range of the poly-Si film was reduced to 3×10^{17} cm^{-3}, and the Ni concentration at the poly-Si/SiO_2 interface was reduced from 4×10^{20} to 5×10^{19} cm^{-3}. In the (VIC + RTA) process, the metal contamination during the VIC process was limited to the poly-Si seed layer. The contaminated metal (Ni) was redistributed during the RTA process, resulting in reduced metal contamination. It is very critical to reduce the leakage current in poly-Si TFTs. The Ni accumulated at the surface might be removed by oxidation and chemical etching.

For the purpose of obtaining a good quality poly-Si film by RTA, a (VIC + RTA) process was introduced. Compared to the RTA process alone, the crystallized temperature was lowered by as much as 50°C. The poly-Si film produced by the RTA process had microstructures such as small grains and irregular plane orientation, whereas the poly-Si film produced by the (VIC + RTA) process presented a needlelike growth front and relatively well-arranged planes. Because of the residual $NiSi_2$ phase in the poly-Si seed layer, the top poly-Si layer appeared to have microstructural characteristics such as those produced by the VIC process even though it was annealed for only 5 min by RTA. In addition, the Ni concentration in the poly-Si film produced by the (VIC + RTA) process is lowered

to 5×10^{19} cm^{-3} at the vicinity of the interface between the poly-Si film and the SiO_2 layer and is lowered to 3×10^{17} cm^{-3} in the middle range of the poly-Si film. As a result, poly-Si film with good quality could be successfully obtained in a short annealing time, while the overall metal contamination in the poly-Si film could be reduced as well. The reduction in Ni concentration in the poly-Si film can greatly reduce the leakage current of the film, which is the main obstacle of using poly-Si TFT for AMOLEDs.

Acknowledgment

This work was supported by the Excellent Research Center program (no. 2008-0062289) and the Priority Research Center program (no. 2009-0094040) through the National Research Foundation of Korea, funded by Korea Ministry of Education, Science and Technology (MEST).

Korea Advanced Institute of Science and Technology assisted in meeting the publication costs of this article.

References

1. E. Korin, R. Reif, and B. Mikic, *Thin Solid Films*, **167**, 101 (1988).
2. C. Hayzelden and J. L. Batstone, *J. Appl. Phys.*, **73**, 8279 (1993).
3. J. H. Ahn, J. H. Eom, and B. T. Ahn, *Sol. Energy Mater. Sol. Cells*, **74**, 315 (2002).
4. J. H. Eom, K. U. Lee, and B. T. Ahn, *Electrochem. Solid-State Lett.*, **8**, G65 (2005).
5. S.-W. Lee and S.-K. Joo, *IEEE Electron Device Lett.*, **17**, 160 (1996).
6. S. I. Jun, Y. H. Yang, J. B. Lee, and D. K. Choi, *Appl. Phys. Lett.*, **75**, 2235 (1999).
7. J. N. Lee, Y. W. Choi, B. J. Lee, and B. T. Ahn, *J. Appl. Phys.*, **82**, 2918 (1997).
8. J. H. Choi, D. Y. Kim, B. K. Choo, W. S. Sohn, and J. Jang, *Electrochem. Solid-State Lett.*, **6**, G16 (2003).
9. B. Pecz, L. Dobos, D. Panknin, W. Skorupa, C. Lioutas, and N. Vouroutzis, *Appl. Surf. Sci.*, **242**, 185 (2005).
10. G. Huang, Z. Xi, and D. Yang, *Vacuum*, **80**, 415 (2006).
11. L. Haji, P. Joubert, J. Stoemenos, and N. A. Economou, *J. Appl. Phys.*, **75**, 3944 (1994).
12. L. Pereira, R. M. S. Martins, N. Schell, E. Fortunato, and R. Martins, *Thin Solid Films*, **511–512**, 275 (2006).
13. J. H. Ahn, J. H. Eom, and B. T. Ahn, *J. Electrochem. Soc.*, **151**, H141 (2004).
14. J. H. Eom, K. U. Lee, and B. T. Ahn, *J. Electrochem. Soc.*, **154**, H194 (2007).